communications earth & environment

ARTICLE

https://doi.org/10.1038/s43247-023-00844-z OPEN

The utility of historical records for hazard analysis in an area of marginal cyclone influence

Adam D. Switzer[1,2✉], Joseph Christensen[3], Joanna Aldridge[4,5], David Taylor[6], Jim Churchill[6], Holly Watson[6], Matthew W. Fraser[7,8] & Jenny Shaw[9]

Shark Bay Marine Park is a UNESCO World Heritage Property located in a region of marginal tropical cyclone influence. Sustainable management of this unique environment as the climate changes requires a quantified understanding of its vulnerability to natural hazards. Here, we outline a structured analysis of novel historical archive information that has uncovered reports of an extreme storm surge associated with a Tropical Cyclone in 1921 that generated remarkable overland flow which left fish and sharks stranded up to 9.66 km (6 miles) inland. Weighted information from historical archives is placed in a new framework and provide inputs to modelling of this event which improves the understanding of its magnitude and furnishes records of the impacts of what occurred on that day and notably also in the years following. The suite of plausible tracks that reproduce the historical data contextualise the storm as a marginal Category 4 or 5 storm and its return interval as equivalent or slightly greater than the current local planning level for coastal flooding in the region. The outcome underscores the global importance of examining the probable maximum event for risk management in areas of marginal cyclone influence where vulnerable ecosystems or vital regional infrastructure of key economic importance are located, and the need to factor in TC risk in marine conservation and planning in the Shark Bay World Heritage Property.

[1] Earth Observatory of Singapore, Nanyang Technological University, Singapore, Singapore. [2] Asian School of the Environment, Nanyang Technological University, Singapore, Singapore. [3] School of Humanities, University of Western Australia, Perth, Australia. [4] School of Geosciences, University of Sydney, Sydney, Australia. [5] Griffith Centre for Coastal Management, Griffith University, Nathan, Australia. [6] Baird Australia, Level 22 227 Elizabeth St, Sydney, Australia. [7] OceanOmics Centre, The Minderoo Foundation, Forrest Hall, Perth, Australia. [8] School of Biological Sciences & Oceans Institute, University of Western Australia, Perth, Australia. [9] Western Australian Marine Science Institution, Perth, Australia. ✉email: aswitzer@ntu.edu.sg

Tropical cyclones (TCs) pose considerable risk globally and examining changes in cyclone risk and determining the causal factors for such changes are vital to adaptation measures for cyclone events[1]. Increasing TC intensities are conventionally thought to be associated with a warming climate[2]. However, confidence in this association is diminished in sites of marginal cyclone influence or in areas where observations of cyclones have been poorly recorded or where available instrumental data is inhibited by poor spatial and temporal resolution[3]. Such limitations cause difficulties in detecting the significance of any intensity trends in observations as these are inherently linked to heterogeneities in the relatively short past instrumental records of TCs. Recent work has increased confidence in projections of increased TC intensity under continued warming[1,2,4].

Future risk at sites of marginally influenced by cyclones. Tropical cyclones are likely to shift poleward in a warming climate[5–7] and some suggest that this trend is particularly obvious in the Southern Hemisphere[8]. Evidence of the poleward shifts in storm tracks have been found in both the reanalyses of the instrumental records[9,10] and projections from numerical models including models with enhanced greenhouse gas concentrations[1,5,8,11–14]. For example, Chang et al.[8] suggest that storm tracks could likely shift poleward between 1° and 2° in latitude on average if CO_2 emissions doubled. A doubling of CO2 level may seem unlikely but 10 years on since the Chang et al.[8], paper CO_2 levels have already increased to more than 420ppm and the rate of emissions continues to rise globally[15]. While several mechanisms have been put forth to explain the poleward shift, there has been little to no consensus on the dominant processes that are driving such a trend[16]. Regardless of the causal mechanism, the poleward migration of TCs is likely to affect areas beyond the traditional TC hotspots. This likelihood underscores the need to build robust and long records of cyclone activity in areas of infrequent cyclone hazard found in cyclone prone ocean basins.

Shark Bay Marine Park. Shark Bay lies on the Western Australian coast at a latitude of 26°S, at the southern edge of TC influence on the eastern margin of the Indian Ocean. Shark Bay is recognised as a UNESCO World Heritage Property as it holds the largest and most diverse seagrass assemblages in the world[17]. The Shark Bay area also provides favourable habitats for marine fauna of high conservation value including dugongs and sea turtles[18,19]. It also has the most diverse stromatolites and microbial mats in the world[20]. The Shark Bay Marine Park (SBMP) is part of the World Heritage Property. Known locally as Gathaagudu (Two Bays), Shark Bay is Australia's largest marine embayment and it consists of two shallow gulfs with an average depth less than 10 m (Fig. 1). The tidal cycle patterns of Shark Bay are mixed diurnal and semi-diurnal with a range of 1.4 m and the bay is oriented in the north-south direction and has a shallow and complex bathymetry[21]. The elongate north-south morphology of the bay demonstrates characteristics that are likely to amplify the magnitude of storm surge during the passage of the rare seasonal TCs.

Currently, research within the context of SBMP are primarily focused on the environmental impacts of extreme events such as the 2010/11 marine heatwave[22–25]. In contrast, TCs and storm surge risk remain relatively understudied despite the threat that TCs place on the status of world heritage values, safety of coastal infrastructure, indigenous cultural values and local livelihoods in a regional economy that is heavily dependent on nature-based tourism[20]. Such ignorance is likely due to the relatively rare occurrence of TC events in the region, as no damaging storm surge event has been recorded since the creation of the SBMP in 1994.

Tropical cyclones in the Shark Bay region. Reliable satellite observations of tropical cyclones in Western Australia began in the 1969/70 season[26]. Over the satellite era, an average of approximately one TC capable of generating winds exceeding gale force or 34 knots occurs every five years in the principal regional town of Denham (Fig. 1)[27]. Recent records of tropical cyclones in the Shark Bay area include TC Seroja (2021), TC Hazel (1979) and TC Herbie (1988)[28–33]. Historical records indicate that several severe TC events have been observed at Shark Bay, notably on 28 February–1 March 1839, 25 February 1893, 24 January 1898 and 11 February 1937, in addition to the event of 17-18 February 1921 reported on here. Beyond historical records, geological studies conducted near Hamelin Pool, southern Shark Bay (Fig. 1) estimate a severe TC frequency of 190–270 years over the Holocene, based on parallel shell ridges nearby[34].

Investigating storm surge histories. Storm surges are extreme sea-level events driven by a combination of strong winds piling water against the coastline and super-elevation of local offshore sea level by lower atmospheric pressure. Storm surges can produce extensive overland flow and coastal flooding on vulnerable coastlines[35,36]. Storm surge risk is typically characterised by the return period or the average recurrence interval (ARI), which is simply expressed as the average time between events of a particular storm surge height. Coastal development on the Western Australian coast requires consideration of a 500-year ARI for coastal inundation events. However, it is difficult to estimate this level from measurements due to the constrained history of cyclone-induced storm surges both temporally and spatially[37]. Limited historical events, together with the paucity of tide-gauge records dating back to the early 20th century, significantly undermine the data available to complete accurate ARI analysis and therefore limit the accuracy of such values. Most ARI analyses use stochastic modelling frameworks that generate a synthetic climatology of TCs and storm surge based on the historical climatology of TC events[38,39]. Assessing the quality of this underlying historical climatology is therefore integral to improving the accuracy ARI analysis.

Historical records can play an important role in the assessment of numerous hazards, as they address an inherent data limitation posed by relatively short, spatially constrained and fragmented instrumental records[40–42]. Here, we examine unique historical records of an intense landfalling cyclone on the Shark Bay coast on 17–18 February 1921. We offer a validation framework for using historical observations and outline a methodology for reconstructing historical storms in settings of marginal cyclone influence.

Integrating pre-instrumental records. In this study we compare a historical record of a major cyclone impact with the best track dataset of the Australian Bureau of Meteorology (BOM). Best-track datasets are widely used in weather and climate applications and they inherently come with a level of uncertainty in terms of TC position and intensity[43,44]. Typically both position and intensity uncertainty decreases as cyclones become more intense as the emergence of an cyclonic eye in satellite datasets allow a greater accuracy for determining the circulation centre[43]. The uncertainty in best-track position and intensity are not trivial and best track datasets should be revisited when new observations from the historical or instrumental datasets come to light or advances are made on how to incorporate different information sources into best track datasets.

The role of palaeoarchives. Considerable research efforts have been put into incorporating prehistoric and palaeo-archives into

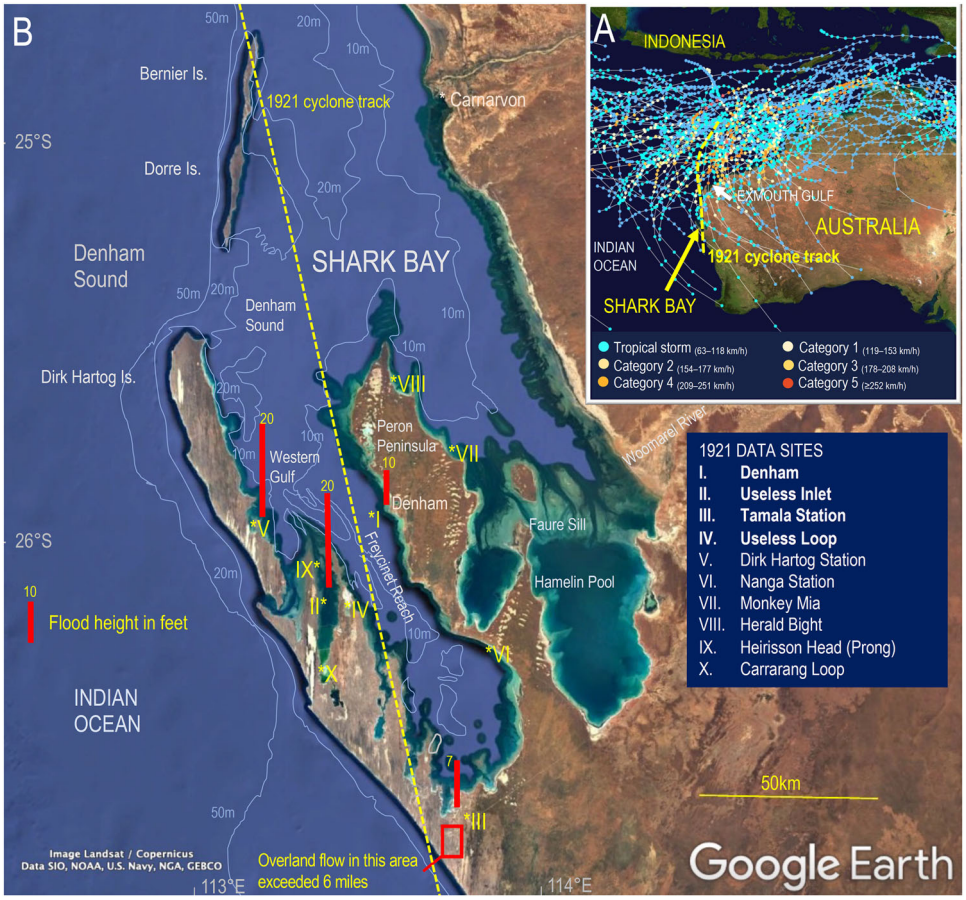

Fig. 1 Maps of the 1921 cyclone track and impacts its Shark Bay, Australia. Historical records of 1921 TC impacts, Shark Bay, Australia. **A** Shows the location of Shark Bay on the West Australian coast along with the cyclone tracks from 1980-2005 from the International Best Track Archive for Climate Stewardship (IBTrACS) database[102]. Field data from Sites I to IV (**B**) were used to constrain the inverse model reconstruction of the storm surge and its impacts. The Bureau of Meteorology best track[27] for the likely 1921 cyclone is marked with a yellow dotted line in both panels **A** and **B**. Panels **A** and **B** use Google Earth with data from SIO, NOAA, U.S. Navy, NGA, GEBCO and images from Landsat / Copernicus.

regional cyclone risk assessments in only a few locations globally[45–47] including a few studies on the West Australian coast[34,48]. Sediment deposits left by storm washover are arguably the most frequently employed proxy for the reconstruction of past storms[45,46] and they can provide centennial- to millennial-length records to examine the frequency of storm surge inundation. However, such proxy records are heavily dependent on coastal geomorphology, hydrodynamic conditions and storm characteristics[49] and record only the most impactful events at a site because only the most intense storm surges leave sedimentary signatures in coastal environments.

Recently high-resolution records capable of annual resolution have become popular and these typically come from geochemical studies of isotopic ratios measured in speleothems[50] or tree rings[51,52]. Tree rings also have the added advantage of applying tree-ring-width derived metrics to produce estimates of tropical cyclone precipitation[53,54]. Highlighting detailed historical records of past storms like that presented here provides a valuable cross-references for high resolution records and contributes to building more robust proxy records.

Results and discussion

Validating historical evidence and reconstructing TC1921. In climate history, historical observations of weather and climate fill a critical gap between instrumental records and long-term paleoscientific datasets[55]. Historical records can provide details about TC events to reconstruct the event through numerical modelling[56–59]. Summaries of tropical cyclones in Western Australia for the pre-satellite era indicated the 1921 event resulted in two deaths and ~£10,000 in lost and damaged infrastructure, mainly affecting the local pearling industry[60,61].

Through an extensive survey of archives at the State Records Office of Western Australia and newspaper reports via the National Library of Australia's 'Trove' database, we uncovered additional evidence of the 1921 TC impacts. Our survey located a detailed, hand written testimony of the 1921 TC by a Pearling Inspector, Mr. Wally Edwards, who witnessed the cyclone and its aftermath. The testimony constituted observations of the cyclone's impacts in the most heavily affected areas of Shark Bay's western gulf, spanning a period of over 6 weeks after the event.

Development of a Quantified Historical Data Framework. The quality of the historical information integrated into the numerical modelling was quantified via a novel Quantified Historical Data Framework (QHDF) where historical accounts were examined using a five-dimensional assessment along axes of 'proximity', 'immediacy', 'accuracy', 'impartiality' and 'provenance' (see methods) that were given equal weighting in terms of importance. The Edwards account stands out as incredibly detailed, consistent and robust and in particular he noted that storm tides were ~3.0 m (10 ft) and ~6.1 m (20 ft) above the highest tide at Denham (Site I) on the eastern bank of Freycinet Reach and at Useless Inlet (Site II) on the western bank respectively. Also of note, Edwards, found that overland flood and inundation peaked at

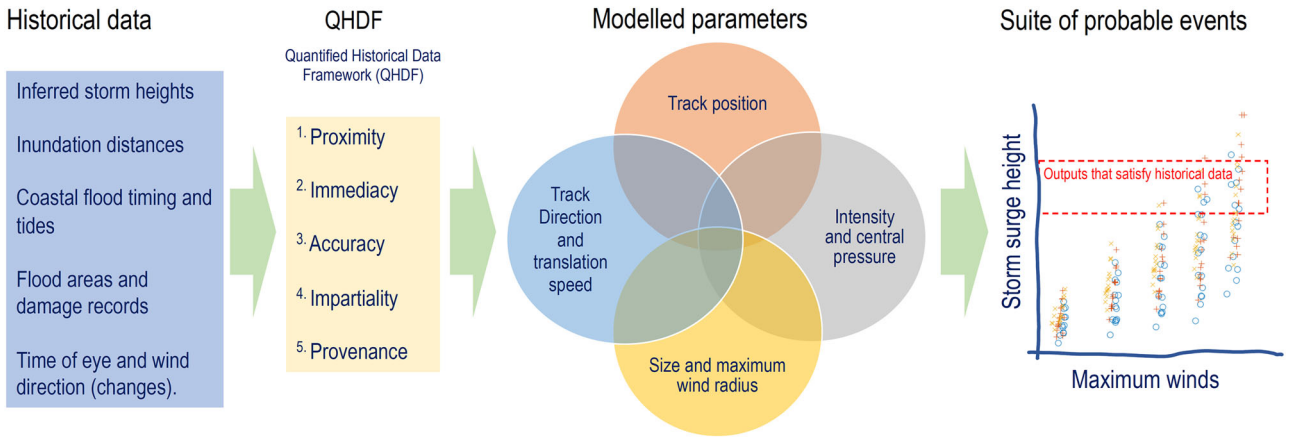

Fig. 2 Methodology to reconstruct cyclones from historical data sources. Schematic figure summarising the methodology to reconstruct historical cyclones that made landfall. The QFHD allows a detailed assessment of the historical dataset and an opportunity to examine the consistency and quality of the historical data used in the reconstructions.

Table 1 Parameters for storm surge modelling and comparative results.

Parameters					Peak surge (m)		
RUNID	**Central pressure (Pc) [hPa]**	**Track position [deg]**	**Orientation at landfall [deg N]**	**RMW [km]**	**Denham (site I)**	**Shark Bay (near Tamala station)**	**Useless loop (site IV)**
BOM	989	0	0	65	0.86	1.28	1.7
115	930	0.4	15	20	3.3	4.1	5.2
164	945	0.2	15	30	3.1	4.2	4.3
165	930	0.2	15	30	3.7	5.0	5.0
180	930	0.2	7.5	30	3.2	4.5	4.3
195	930	0.2	0	40	2.5	4.2	6.5

Model results and track parameters satisfying the observed wind and surge. Track position and orientation at landfall given relative to the Bureau of Meteorology Best Track (labelled BOM).

~2.1 m (7 ft) above ground level at Site III at the southern end of Freycinet Reach near Tamala Station (Fig. 1). Near site III, Edwards also found sharks and fish that were stranded up to 9.66 km (6 miles) inland – a clear note on the probable extent of overland flow in the area. In addition, Edwards observed ship groundings, inundated coastal wells, flooding and altered coastal geomorphology at other locations in Freycinet Reach and Freycinet Estuary (Fig. 1 and Supplementary Table 1). Evidence of longer-term socio-economic and environmental impacts was also collated from archival sources (Supplementary Table 2) to facilitate comparison to documented impacts of more recent TC events.

Supplementary information from nearby vessels. Meteorological reports published after the event indicate that at least three vessels likely made observations of the 1921 cyclone off the Western Australian coast. The SS Toromeo, southwest of Fremantle, on 19 February; and the SS Great City and SS Carignano, west of Shark Bay on 18–19th February[62]. These vessels are the likely source of the instrumental meteorological observations extracted from the International Comprehensive Ocean-Atmosphere Data Set (ICOADS; Supplementary Fig. 1). Of note a minimum surface pressure of 988.5 hPa was observed by one ship (name not stated) ~300 km west of the inferred TC at 01UTC on 18 February 1921. This further implies that the storm was of much greater intensity and size than previously suggested.

Inverse modelling for storm reconstruction. We used numerical models to reconstruct the 1921 TC and investigated whether the elevated water levels and inundation described in the historical records could be replicated. We use a non-linear, inverse modelling approach akin to a grid search model with elements of brute-force as directed by the historical data. Storm surge levels in estuaries and semi-enclosed bays are highly sensitive to changes in TC parameters such as the central pressure, angle of approach to the coastline, forward speed and radius of maximum winds (RMW)[63–66]. For example, a change in the angle of approach to the coastline of 10–15° has been reported to give >0.5 m variation in the storm surge magnitude[67]. If the angle of approach of the 1921 cyclone aligned with the NNW-SSE orientation of the longitudinal axis of Shark Bay this would likely amplify storm surge at the southern end of the bay (Fig. 1). The aim of the modelling exercise is to estimate probable combinations of TC track parameters that resulted in the historical observations of storm tide inundation, and thus establish the likely intensity and category of the 1921 TC based on a suite of model outputs that meet the field data (Fig. 2).

A set of 225 numerical simulations were conducted, firstly using the track specified by the Australian Bureau of Meteorology (BOM) Previous Tropical Cyclones: The Australian Tropical Cyclone Database[27] of the 1921 TC (Fig. 1B and Table 1). Then we model a set of cyclone tracks with varying forward speeds, RMW, angles of approach and track positions (Supplementary Fig. 2 and Supplementary Table 4). This exercise can be considered as an expert-guided, non-linear, inverse modelling approach (Fig. 2), whereby the underlying distribution of each cyclone track parameter is informed firstly by the archived cyclone track, then varied within feasible ranges constrained by the historical observations.

The test set of cyclone tracks representing the 1921 TC consists of 225 tracks (Supplementary Table 4), which are made up of

combinations constructed from; five central pressures, three radius of maximum winds (RMW), three different orientations of track at landfall, and five track positions (shifting westward by 0.1° from the position of the BOM best track). The eye of the cyclone was also shifted backward along the track to reflect the changes in RMW while maintaining the timing of the onset of north-easterly winds at Denham noted in the historical record of Edwards. Shipboard observations from historical accounts indicate extended gales offshore, so the radii of gales were set to be 400 km for all test tracks.

We simulated cyclonic wind, and pressure fields using a parametric model[68]. The model utilises TC track information such as central and ambient pressures and radii of maximum winds and gales. For storm surge modelling we applied Baird's southwestern Australia ocean model[69,70] that is constructed in the unstructured mesh open source 2D-vertical hydrodynamic model Delft3D-FM[71–73] (see "Methods" section; Supplementary Fig. 2A, B). Baird's model has been previously calibrated for the astronomical tide and validated for 35 historical TC storm surge events Australia-wide, and it was able to replicate measured peak tidal residuals with a linear fit of 0.9957 ($R2 = 0.96$)[70]. We note that our study does not consider the contribution of waves to elevated coastal water levels via wave set-up as a component of run-up processes. The wave environment of the Shark Bay Gulf would be depth limited due to the shallow water where wave breaking in such energetic conditions occurs offshore and thus limit the contribution of waves to the coastal flood heights noted. The wave set-up from wave breaking across the bay is likely to increase water levels at tide gauge locations in the order of 0.1–0.2 m as found for similar environments and cyclonic conditions (e.g., close by in Mermaid Sound, Western Australia (Churchill et al.[73]), and also Moreton Bay, Queensland[74,75].

The quality of the historical information integrated into the numerical modelling was quantified using the five-dimensional assessment of our QHDF. Using the QHDF, the observations by Edwards and other observers at Denham were prioritised, followed by the observations made by Edwards at Tamala station (Site III), and followed by accounts of inundation at Useless Inlet (Site II) and at other locations (Supplementary Table 5).

Our numerical simulation of the 1921 TC BOM Best Track (Fig. 1 and Supplementary Fig. 2D) does not replicate the extreme storm surge around Shark Bay that was observed in the historical records. Simulated peak storm surge using the 1921 TC BOM Best Track was only 0.86 m at Denham and 1.28 m at the landfall location, falling short of observation data by more than 50% (Table 1).

Results from the numerical simulation of 225 scenarios indicate that there is considerable variability in storm surge magnitude when subjected to variations in the TC track parameters at Denham (Site I) and at landfall (Fig. 3). Of the 225 simulated scenarios, 29 satisfy the constraints of the historical observations at Denham only including peak winds from the northeast quadrant exceeding gale force (34 m/s), and peak water level at spring tide >3 m (10 ft; Fig. 3). Adding the constraints at Useless Loop (Site IV) and at landfall north of Tamala Station (Site III) narrow the number of storm scenarios that match the historical record to five (Table 1).

Results from our numerical modelling indicate a likely central pressure for the 1921 TC in the range of 930-945 hPa corresponding to a Category 4 or borderline Category 5 TC. This is of a much greater intensity than that implied by the BOM Best Track record with a Pc of 989 hPa (Table 1). It also suggests the 1921 TC storm surge is on par with Cyclone Vance which passed across Exmouth Gulf ~450 km North of Denham in 1999[76–78] but it was likely not of such intensity (Vance was 910 hPa)[30]. The 1921 storm was also likely of similar intensity and impact to Cyclone Yasi, which struck in central Queensland on the northeast Australian coast in 2011[78].

A key finding is that this ranks this storm as the most intense event to be recorded in the Shark Bay region compared to the BOM Best Track archive[33] and the most intense TC event recorded in Western Australia south of 25°S. In Western Australia 25°S is an important geographical boundary, as this is where the state building code regarding winds changes to Region C (lower risk) from Region D to the North[79]. This implies that the risk posed by cyclonic winds south of 25°S may also be underestimated.

Figure 4 shows the model results for Run 180, one of the 5 model runs most consistent (Table 1) with the historical observations. This example (Run 180) reproduces a storm surge at Denham of 3.2 m + 0.8 m high tide, which gives a total water level above MSL of 4.0 m – consistent with the observed inundation height of between 2.1 m (7 ft) and 3.05 m (10 ft), with very low elevation of 2–3 m MSL at the low lying Denham coastal foreshore. All runs presented in Table 1 are consistent with the account of Edwards, who records that the flooding occurred at the top of spring tide. The eye of the storm in all 5 model scenarios did not pass through Denham, which is again consistent with the historical accounts.

One notable constraint is the historical observations of overland flow and stranded fish extending 6 miles inland at Tamala Station at the south end of Shark Bay (Fig. 1 and Supplementary Table 1). The landscape around Tamala Station is dominated by North-South oriented, low-relief dune field, as indicated by the striations on the satellite imagery and described by Playford et al. [31]. Cursory analysis of the STRM topography satellite imagery and Google-StreetMap (Supplementary Fig. 3) indicates that areas of low-lying land with elevations <6 m could be connected well inland beyond Tamala Station. We did not model overland flow due to the lack of quality elevation data in this very remote location. However, our results show that the elevated water level was likely ~6 m above mean sea level near the coast at the southern end of the Gulf near Tamala Station (Site III). Currently we were unable to model whether a storm tide of this magnitude could propagate the observed distance inland as this is beyond the scope of this project and this is noted as a limitation and avenue of future research. However, we interpret from the geomorphology that given the north-south, shore normal orientation of the low relief dune field it is likely that a storm surge exceeding 5 m could funnel this far inland (Supplementary Fig. 3). Further, the scale of the storm surge likely caused considerable modification to the soft coastal landforms through sediment transport processes, destroying dunes and cutting new channels. Coupled hydrodynamic – sediment transport modelling is also beyond the scope of this study for this historical event given very limited observational data.

We contextualise the severity of the 1921 TC relative to current planning levels for Denham where the 100 year ARI level for existing development is 3.6 m above Australian Height Datum (AHD) (which includes 0.9 m Sea Level Rise allowance), and the 500 year ARI level for new freehold development is 4.2 m AHD as required by State Planning Policy 2.6. These levels were determined via simulation of 1000 years of synthetic TC tracks (154 events) impacting Shark Bay based on the TC climatology since 1960[80]. Subtracting the Sea Level Rise allowance gives a 500-year ARI storm tide of 3.3 m, which is equivalent or slightly lower than the observed water levels from the 1921 TC. This result implies that either the TC climatology and hence the planning level is underestimated, or that the 1921 TC event was an extreme outlier in terms of recurrence interval. This is likely important for both surge and wind risk and can be tested by expanding the TC climatology underlying the synthetic TC track set, which currently only spans the satellite era (post 1969/70).

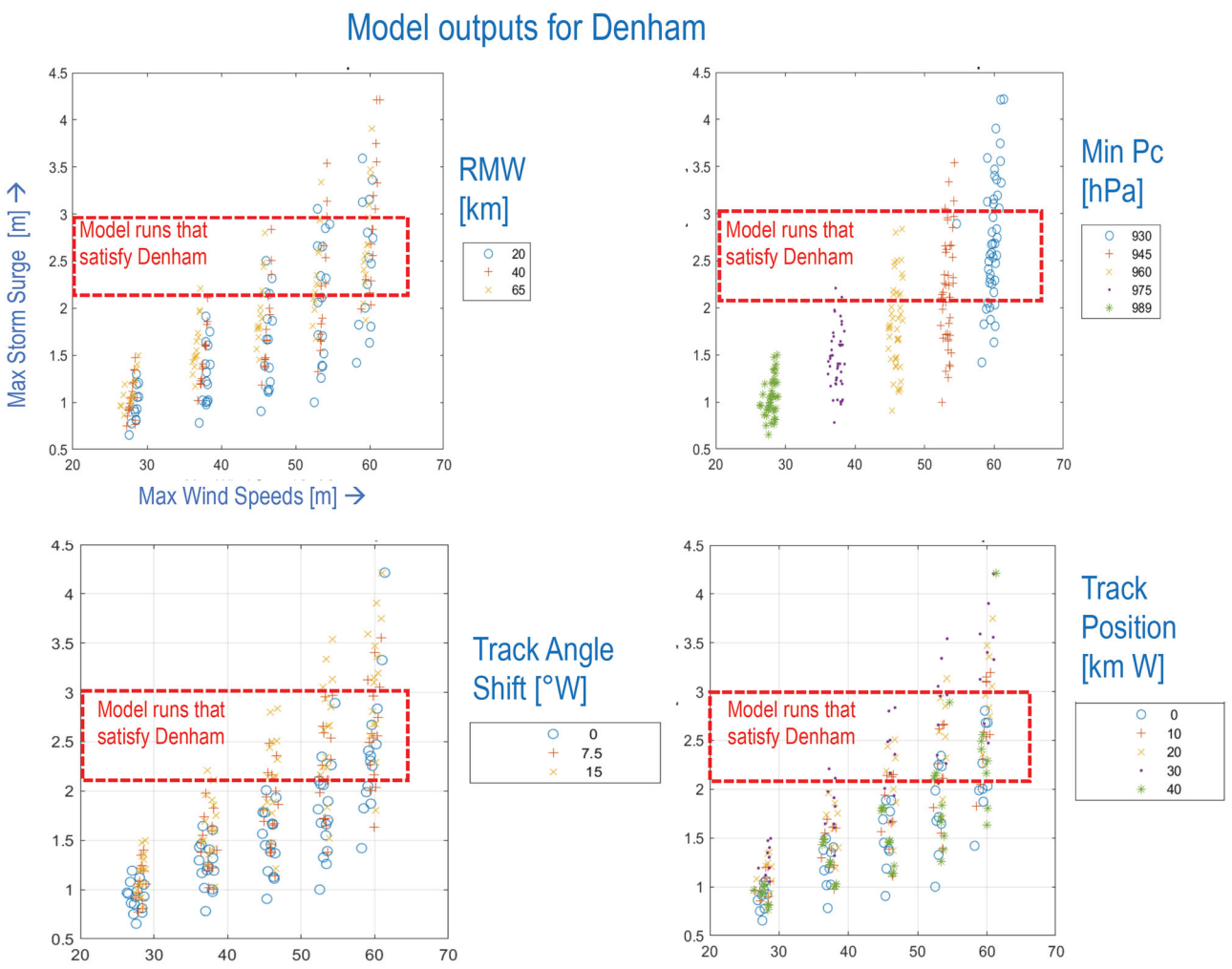

Fig. 3 Analysis of the 1921 TC with a non-linear, inverse modelling approach. Model Outputs of maximum wind speed vs peak storm surge at Denham (Site I) for variants of the 1921 TC BOM Best Track: Central Pressure, Radius of Maximum Winds, Orientation at landfall, Track position. Collectively 29 scenarios match the historical records at Denham.

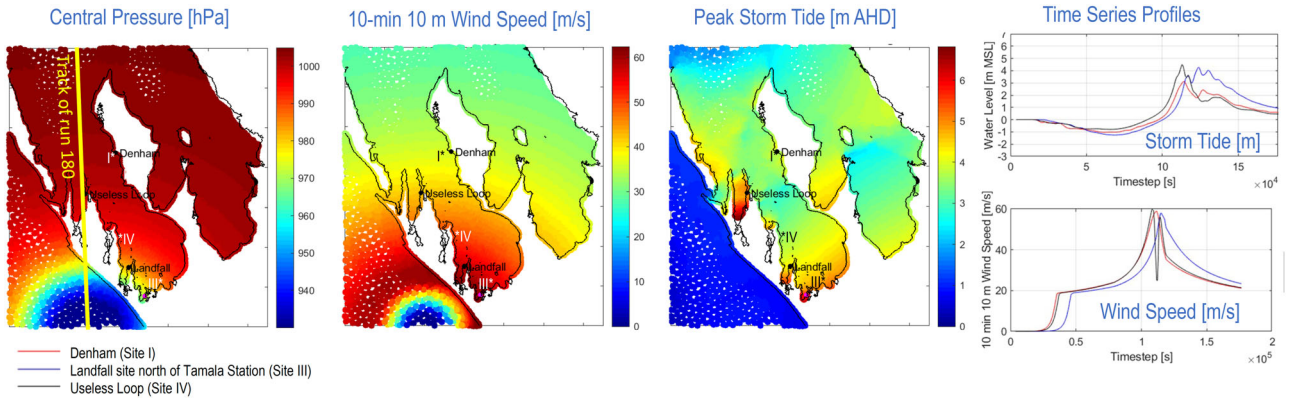

Fig. 4 Modelled storm surge suggests category 4-5 cyclone impacts. Model results for Run 180. This model is one of five consistent with the historical observations, at Denham of water level above 3 m mean sea level and consistent with the observed inundation of between 2.1 m (7 ft) and 3.05 m (10 ft) over land. The model also reproduces the extremely high storm surges at Useless Loop (Site IV) and at landfall north of Tamala Station (Site III).

How intense was TC1921 and how does it compare to other events regionally? The 1921 TC was clearly more intense than a Category 1 or 2 event that was indicated in Bureau of Meteorology records. Our numerical modelling indicates that the 1921 TC was likely a borderline Category 4–5 event. The 1921 TC event at Shark Bay is likely comparable to a similarly intense TC Yasi which crossed the north Queensland coast in 2011. TC Yasi had a minimum central pressure of 929 hPa and generated a storm surge of 5.3 m at Cardwell on the Queensland coast[78]. Our modelling of the 1921 TC, indicates a likely storm surge at Denham of ~3.0 m on top of a spring tide to a water level of ~4.0 m. This figure far exceeds the flooding recorded during TCs

Table 2 Uncertainties considered in storm surge modelling of the 1921 cyclone.

Source of uncertainty	Contributing processes	Estimated error in peak storm surge magnitude (RMSE)	Validation
Observation error	Inaccuracy in historical accounts, lack of timeliness in recording recollections.	~0.3 m	Cross-checking of various sources, use of QHDF framework to prioritise observations.
Mean sea level variation	Seasonal and interannual fluctuations, SLR	~0.2 m	Lowe et al. [100]
Hydrodynamic model	Bathymetry, bed roughness, wind drag coefficient	0.18 m	Tide (local), TC events – Australia wide
Parametric wind model	Wind Pressure Relationship, second order variations in inflow angle.	~0.2 m	Vijayan et al. [101]
Nearshore wave processes	Wave set-up, wave-current interaction	~0.2 m	Depth limited wave environment.
Sediment transport processes	Dynamic changes in bathymetry and topography, long term evolution of bathymetry since 1921	~0.1 – 0.2 m	Inferred without validation

Table of uncertainty sources considered in the storm surge modelling. The sum of all sources is around 1 m though each source is likely randomly distributed and would likely reduce by interaction. We find that a combined RMSE of 0.2–0.3 m is more likely.

Hazel (~1.9 m AHD) and Herbie (~2.4 m AHD)[80]. The modelled 1921 TC storm surge is also comparable to the storm surge experienced at Exmouth Gulf (Fig. 1) during the passage of TC Vance in 1999, where a peak water level of 3.6 m above local datum was recorded inside the town's marina[77]. A repeat of the 1921 event today would likely have devastating consequences considering substantial foreshore development in Denham since 1988, and, in the context of high climate change risks to key World Heritage values within the SBMP[20,81].

Discussion of limitations, uncertainties and avenues of future research. The core purpose of the storm surge modelling undertaken in this study is to aid in the interpretation of the range of likely intensities of the 1921 TC event, not to fully replicate the complex hydrodynamic-wave and sediment transport processes that likely occurred. More detailed and complex coupled process modelling is left to future research. Sources of uncertainty in the peak storm surge magnitude and relationship with the cyclone intensity are discussed in the methods section and summarised in Table 2. The cumulative impact of these sources of uncertainty does not strongly influence the conclusion of this study, as the error from each source would be randomly distributed and could cancel each other out, and it is highly unlikely that all sources of error during this event would have contributed to their maximum extent (an estimated 1 m in total). A combined RMSE of 0.2–0.3 m is more likely, which would not considerably change the estimation of the event intensity in this regard.

Long-term impacts of TC1921 imply considerable sustainability issues. Notably, the 1921 TC also had considerable long-term socio-economic and environmental implications, that were reported for up to 30 years after the event[82]. For example, Denham experienced saltwater inundation of its freshwater wells, which remained saline into the early 1950s in a context where the availability of freshwater was a major limitation on regional economic development[81]. Pastoral stations on Peron Peninsula (Fig. 1) suffered livestock losses due to inundation of coastal wells (bores). The pearling industry was impacted by short-term declines in *Pinctada albina* populations, and longer-term, by slow recovery of stocks (Supplementary Table 2). At Shark Bay, *P.albina* is interspersed with dominant seagrass assemblages[82]. A contemporary source suggests dugongs were also encountered less frequently in the years following the 1921 TC (Supplementary Table 2).

The ecosystem damage noted from the 1921 TC is consistent with reports elsewhere from recent events. For example, TC Yasi in 2011 provides a contemporary example of the impact of TCs have on seagrasses and dugong populations. Yasi damaged 98% of tropical intertidal seagrass meadows in northern Queensland waters[83,84], and caused biomass and shoot density declines in surviving meadows[85]. The seagrasses in Queensland were primarily classed as colonising species, which would be expected to have a lower persistence but faster recovery rate following disturbance events than the persistent seagrasses that dominate Shark Bay[86]. Cyclonic-driven loss of seagrass habitat coincided with declines in the estimated dugong population in the Southern Great Barrier Reef Region[87], and similar patterns have been noted in Shark Bay following climate-driven seagrass loss[88]. Cyclone related loss of seagrasses in Shark Bay would have considerable long-term knock-on effects to ecosystem functions and services, particularly as the seagrasses of Shark Bay contribute to several World Heritage values.

What would a similar cyclone do in Shark Bay today? Using a comparison of the storm surge magnitude against the local topography in a first-order bathtub approximation of inundation extent, a storm surge exceeding 2 m at Denham today would likely inundate the main street along the foreshore and flood critical infrastructure, including the shire headquarters, key state government offices, a World Heritage Discovery Centre, most of the town's grocery stores, petrol stations and restaurants, tourist accommodation, and the town jetty as well as the boat launching facility[81]. This would be devastating to the regional tourism economy that is estimated to be bring in $64 million per year in visitor expenditure[20]. A solar salt facility at Useless Inlet, which contributes approximately $40 million per year[20] to the regional economy, would also be threatened by a storm of similar magnitude to the 1921 event.

Regional cyclone risk in the future. Another important consideration is the impact of climate change on the SBMP and the surrounding region. Gradually warming Sea Surface Temperatures (SSTs) and episodic extreme weather events such as marine heatwaves will increase heat stress and enhance vulnerability of the temperate seagrasses (*Amphibolis antarctic* and *Posidonia australis*) that already exist at the high temperature limit of their thermal tolerance limits within Shark Bay[23]. Habitat-forming species like seagrasses are particularly vulnerable to synergistic stressors occurring in the same time and place. This was

exemplified within the SBMP during the marine heatwave of 2011, where meadows adjacent to the flowing Wooramel River (Fig. 1) were amongst the worst impacted due to the combination of high temperatures and low light availabilities due to river flooding and inputting fine sediments into the surrounding area[23]. The combined threat posed by marine heatwaves, increasingly frequent and intense storms and sea level rises has led to Shark Bay receiving the highest rating of vulnerability according to the Climate Change Vulnerability Index, a recently-developed methodology for assessing climate change impacts across World Heritage sites[89].

How will TC climatology affect future risk? Regional TC climatology is likely to change with climate change (IPCC 2021) with a poleward shift in the latitude of maximum intensity of tropical cyclone development as SSTs warm and the duration of TCs increases[90,91]. Kossin et al. [90]. found the South Indian Ocean basin has experienced an 18% per decade change in major TC intensity (Saffir Simpson Categories 3–5) exceedance probability based on analysis of a homogeneous 39-year-long global satellite record from 1979 to 2017. Using dynamical downscaling comparing the historical period (1965-2014) with RCP8.5 (2045-2094), Cattiaux et al. [7], investigated potential changes in TC climatology in the southern Indian Ocean. They found a 20% decrease in frequency, and a shift in lifetime maximum intensity from lower to higher categories. They also found a slight poleward extension of the TC tracks of approximately 1° over 80 years. Their finding of a possible shift in the timing of the TC season towards the latter half of the season (Feb–April) could also mean TC events have a greater probability of coinciding with the highest (king) tide events.

Environmental managers must consider TC's within a suite of potential climate stressors for the seagrass meadows and the greater marine ecosystem within the SBMP. The importance of the marine ecosystem mean that any large cyclone will likely have strong potential to erode ecological resilience and directly impact World Heritage values.

Conclusions

This study highlights the risk posed to communities on the margins of TC influence where rare cyclone events in the 100–500 year ARI range, and beyond, are difficult to assess. We demonstrate the clear value of enhancing quantitative risk management methods with multiple lines of evidence offered by historical archives to understanding long term tropical cyclone climatology and storm surge hazard. Such an approach has important implications for land use planning, emergency management and environmental management of this unique World Heritage Property and other sites of marginal cyclone influence. Historical observations provide a key resource for planning and management and an extension to TC climatology that should be utilised for planning and sustainability programmes where possible.

Methods

Development of the Quantified Historical Data Framework. For weather and climate studies, historical data fill a critical gap between instrumental records and long-term paleo-scientific datasets[55]. Historical records can provide details about TC events to reconstruct the event through numerical modelling[59]. Summaries of tropical cyclones in Western Australia for the pre-satellite era indicated the 1921 event resulted in 2 fatalities and ~£10,000 in lost and damaged infrastructure[60]. We surveyed the archives at the State Records Office of Western Australia and newspaper reports via the National Library of Australia's 'Trove' database and uncovered additional evidence of the 1921 TC impacts not previously noted. Our survey located eyewitness accounts in the form of letters, diary entries, memoirs and oral history interviews, at multiple points across Shark Bay. The historical information integrated into the numerical modelling was quantified via a QHDF, drawing on key methods, concepts and findings in historical climatology and historical tempestology. Historical observations are produced by individuals and their interpretation is content-specific; 'To assess and interpret these sources, 'researchers need to know who produced them, why, and how they recorded meteorological conditions and their human consequences'[55]. A 'source-critical' approach to identify human bias, cross-check data from various sources and avoid the repetition of errors in secondary sources is therefore generally applied in historical climatology[92]. As singular weather phenomenon, cyclones and storm surges raise additional questions of reliability in observational records. In their appraisal of available evidence relating to TC Mahina (Qld, 1899), Nott et al. [93] demonstrate the veracity of first-hand observations by known individuals at the time of the event itself, over second-hand or anonymous accounts produced after the event. On the other hand, Christensen[61] has noted a tendency for cyclone impacts to be exaggerated by eyewitnesses affected by confusion, shock or grief in the immediate aftermath of severe events. To address these issues, we adapt Kelso and Vogel's[94] qualitative three-point 'confidence rating' of narrative accounts of drought to distinguish verified, reliable data in historical reconstructions of weather and climate[95] to a five-dimensional assessment of observed cyclone and storm surge impacts. Our QHDF applies a confidence rating of 1 (observation is questionable), 2 (observation is unverified in other sources) or 3 (observation is verified by others), along axes of 'immediacy' (was the observation made during the event, or in its aftermath), 'proximity' (is it first-person or second-hand), accuracy (are there precise and consistent reference points), objectivity (can bias be detected, by way of shock, fear or grief, etc), and provenance (can the observer be identified as a known historical individual). We assume equal weight for each variable and the detailed results are listed in Supplementary Table 5.

Storm surge modelling: model description. The southwestern Australia ocean model used in this study is part of Baird's Australia-wide suite of models[70] constructed in the open source 2D-vertical hydrodynamic model Delft3D-FM[71,72]. The model domain extends from 19.1°S to 35.72°S and 107.6°E to 115°E (Supplementary Figure 2) an area that contains the whole track of the 1921 cyclone. The unstructured model mesh (Supplementary Figure 2) has a maximum 1 km resolution between the −10 m depth contour and the coastline, and finer resolution in complex areas, 3 km resolution between −100 m and −10 m depth and 8–20 km resolution beyond −100 m depth. The model bathymetry is interpolated from available hydrographic data, extracted from Australian Navy Electronic Navy Charts[96]. The model output points were specified throughout Shark Bay at depths ranging from −0.85 to −19.85 m.

Storm surge modelling: model calibration. To calibrate the model the ocean boundaries were forced with TOPEX-8 tidal constituents[97], and compared to year-long tidal calibrations from the Australian National Tide Tables at the nine Australian Standard Ports. Calibration was within the model domain is excellent with a mean amplitude error of 0.02 m or less and phase error of 2.5° for the top eight constituents across all sites. At Denham (Supplementary Table 4) the tidal calibration for a full-year simulation for the year 2011 achieved an RMS error of 0.064 m and model bias of 0.021 m.

Storm surge modelling: model validation. Storm surge from the 1921 Shark Bay TC was reproduced using the Delft3D-FM ocean model, with input parameters from cyclonic wind and pressure fields. The simulations were conducted on the Microsoft Azure™ cloud supercomputer. Cyclonic wind and pressure fields were simulated using the parametric description of ref. [68], which assumes the relative uniformity of cyclonic winds. The parametric model uses cyclone track information including the central and ambient pressure, radius to maximum winds (RMW) and radius to gales (R34) (Supplementary Fig. 3)[68]. To account for the asymmetric nature of cyclones where the forward speed of the system increases the wind speed on one side, the forward speed correction, α, of Shea and Gray[98] was made to the gradient wind speed. Also, an inflow angle correction, β, was made to represent the cross-isobaric flow due to surface friction[99]. The Australian ocean models used here were validated for 35 historical storm surge events[70], replicating measured peak tidal residuals with a linear fit of 0.9957 ($R2 = 0.96$) (Fig. 5 in Burston et al.[70]).

Storm surge modelling: experimental design. The test set of cyclone tracks representing the 1921 Shark Bay tropical cyclone consists of 225 tracks (Supplementary Table 4), made up of a combination of five central pressures, three radius of maximum winds (RMW), three orientation of track at landfall, and five track positions (shifting westward by 0.1° from the position of the BOM best track). The first track is the BOM best track. The 225 storm track variations of the BOM best track were derived by adjusting the track's parameters while making sure that these parameters were still consistent with the historical accounts (Table 1). The variations in RMW also vary the forward speed, as the eye of the cyclone was shifted backward along the track to reflect changed RMW while maintaining the timing of the onset of north-easterly winds at Denham. The historical accounts indicate that gales were quite extended based on ship board observations, so the radius to gales was set to be 400 km for all test tracks. The model can be considered non-linear, inverse modelling approach akin to a grid search model with elements of brute-force as directed by the historical data. Thus each scenario is constrained by a variety of variables tied to the historical information of time, location and storm surge height.

Storm surge modelling: sources of modelling uncertainty. The track intensity and other track parameters are the main source of uncertainty in the estimation of the peak storm surge and are the subject of this investigation. Other sources of uncertainty include those in the hydrodynamic model, including the model bathymetry, bed roughness and wind-drag coefficient, and additional processes such as wave set-up, wave-current interaction, inundation and dynamic sediment transport processes.

Storm surge modelling: cyclone track and parameterisation. Several aspects of the wind field parameterisation can add a second or third order degree of uncertainty to the estimation of the wind speed and hence storm surge magnitude. The modelled synthetic TC tracks were varied at the 12 hourly time step of the Best Track record, as no higher temporal resolution information is available in the pre-satellite era. The track may have varied at finer time steps leading to local changes in behaviour. However, in this region of southwestern Western Australia, south-westward landfalling TC tracks are typically 'captured' systems[32], and exhibit linear behaviour due to the strong prevailing steering winds guiding their track and generating high forward speeds characterised by rapid acceleration associated with a westerly frontal system.

Storm surge modelling: wind-pressure relationship. The relationship of central pressure (Pc) with peak wind speed is determined in the Holland et al. [68] model using the parameter 'bs', which has been found to fit well for the Western Australian region in comparison to BOM post-satellite observations of Pc and maximum sustained windspeeds. In this experiment, a range of values of Pc is prescribed and used to construct a wind field. Any individual cyclone can vary in its peak wind speed relative to its central pressure, and this scatter introduces a degree of uncertainty in the resultant storm surge magnitude, as the wind speed forces the water surface. The authors estimate the range of uncertainty for the peak storm surge magnitude due to this scatter to be in the order of 0.2 m

Storm surge modelling: mean sea level. Lowe et al. [100] show that seasonal and interannual sea level variability can add to the coastal sea level along the West Australian coastline, although this is a second order effect relative to a 4 – 6 m storm surge. The modelling was performed on high tide as this was observed at the time, and no seasonal component was included given the age of the event, although this may have contributed up to 20 cm to the mean sea level at the time. This is within in the uncertainty of the observations of peak water levels which were approximated to the nearest foot. Also, as storm surge develops to a higher magnitude on shallower water, so use of the high tide water level is somewhat conservative.

Storm surge modelling: hydrodynamic model. Unfortunately, a lack of measurements at this site mean that the hydrodynamic model could not be well verified for a recent cyclone event. The tide was well replicated, suggesting that the bathymetry and parameterisation of the hydrodynamic model such as the bed roughness were suitable. Simulations of TC Hazel (1979) and Herbie (1988) (not shown) give storm surge magnitudes at Denham comparable to visual observations of on-ground inundation from unverified sources considering the poor quality of the TC track information for these events, which precludes their use as strict calibration events[100]. The wind drag coefficient was validated comparing a set of 35 modelled historical TC events against good storm surge observations around Australia[69].

Storm surge modelling: bathymetry. An assumption that the bathymetry of Shark Bay as represented in the model was applicable in 1921 is made in the modelling in this study. It is a reasonable assumption, though we recognise that the location of sand shoals has likely changed. The usually low to moderate oceanographic conditions would lead sand shoal evolution towards their equilibrium state in the intervening 100 years. The overall volume of water contained within Shark Bay and average depth is likely to have not varied considerably. The location of particular local shoals is not likely a strong control on peak surge development as the extreme currents would likely rapidly erode them.

While the local sediment distribution in Shark Bay may have changed since 1921, its large scale configuration as a northward open funnel remains. Sediment would also have moved considerably in the event itself given the strong forces exerted by the cyclonic currents and waves. It is likely that extreme wind stress forcing during the 1921 cyclone would have produced a very large storm surge regardless of local sediment patterns at the time and the event would have forced large scale sediment transport to align the sediment with the hydrological forcing. The uncertainty in peak water level introduced from bathymetric change in sedimentary material would be in the order of 10–20 cm.

Storm surge modelling: waves. The wave environment is assumed to be depth-limited in this shallow water environment under cyclonic wave conditions, meaning that wave breaking occurs well offshore and thus contributes to wave set-up on the scale of the whole inlet as opposed to locally against the shoreface. It is estimated that wave set-up may contribute 0.1–0.2 m to the water level across the inlet as found in similar locations in cyclonic conditions (e.g., Mermaid Sound, Western Australia)[70]. This assumption may be tested in a future study using a combination of phase-averaged wave model coupled with a nearshore 2D wave profile model like XBeach. A limitation in this case is that no wave observational data is available in this location for any contemporaneous events for model calibration or validation.

Storm surge modelling: inundation. Inundation modelling was precluded for this event by a lack of high resolution topographic data and it would be informative to understand how a storm surge of this magnitude propagates overland when such data becomes available, Further, coupled hydrodynamic – sediment transport modelling in a future study may inform how large scale changes in bathymetry and coastal landforms may occur during an extreme cyclone event.

Data availability

The data used in this study include historical archive data available from the State Records Office of Western Australia, the State Library of Western Australia, and via the National Library of Australia's 'Trove' digital newspaper database. The Wally Edwards diary and correspondence, and the reports of longer-term impacts derive from records held by the State Records Office of Western Australia (see State Records Office (www.wa.gov.au)). The Ines Fletcher and GW Fry observations derive from collections at the State Library of Western Australia (State Library of Western Australia (slwa.wa.gov.au)). All newspaper reports derive from the National Library of Australia's 'Trove' digital newspaper database, which is open public access (About | Trove (nla.gov.au)). For the State Records Office and State Library, the relevant materials are not accessible online but rather as physical items that must be viewed in person but they are open public access records in this sense.

Code availability

For storm surge modelling we applied Baird's southwestern Australia ocean model (refs. [69,70]) an unstructured mesh open source 2D-vertical hydrodynamic model Delft3D-FM (https://oss.deltares.nl/web/delft3dfm). The Baird southwestern Australia ocean model is commercially restricted though the authors will accept requests for the component related to this project.

Received: 20 December 2021; Accepted: 12 May 2023;
Published online: 31 May 2023

References

1. Kossin, J. P., Knapp, K. R., Olander, T. L. & Velden, C. S. Global increase in major tropical cyclone exceedance probability over the past four decades. *Proc. Natl. Acad. Sci. USA* **117**, 11975–11980 (2020).
2. Knutson, T. et al. Tropical cyclones and climate change assessment: part II: projected response to anthropogenic warming. *Bull. Am. Meteorol. Soc* **10**, E303–E322 (2020).
3. Lin, N., Marsooli, R. & Colle, B. A. Storm surge return levels induced by mid-to-late-twenty-first-century extratropical cyclones in the North-eastern United States. *Clim. Change* **154**, 143–158 (2019).
4. Torres-Alavez, J. A. et al. Future projections in tropical cyclone activity over multiple CORDEX domains from RegCM4 CORDEX-CORE simulations. *Clim. Dyn.* **57**, 1–25 (2021).
5. Bengtsson, L., Hodges, K. I. & Keenlyside, N. Will extratropical storms intensify in a warmer climate? *J. Clim.* **22**, 2276–2301 (2009).
6. Wu, Y., Ting, M., Seager, R., Huang, H. P. & Cane, M. A. Changes in storm tracks and energy transports in a warmer climate simulated by the GFDL CM2. 1 model. *Clim. Dyn.* **37**, 53–72 (2011).
7. Cattiaux, J., Chauvin, F., Bousquet, O., Malardel, S. & Tsai, C. L. Projected changes in the Southern Indian Ocean cyclone activity assessed from high-resolution experiments and CMIP5 models. *J. Clim.* **33**, 4975–4991 (2020).
8. Chang, E. K., Guo, Y. & Xia, X. CMIP5 multimodel ensemble projection of storm track change under global warming. *J. Geophys. Res. Atmos.* **117**, 1–19 (2012).
9. Daloz, A. S. & Camargo, S. J. Is the poleward migration of tropical cyclone maximum intensity associated with a poleward migration of tropical cyclone genesis? *Clim. Dyn.* **50**, 705–715 (2018).
10. Sharmila, S. & Walsh, K. J. E. Recent poleward shift of tropical cyclone formation linked to Hadley cell expansion. *Nat. Clim. Change* **8**, 730–736 (2018).
11. Yin, J. H. A consistent poleward shift of the storm tracks in simulations of 21st century climate. *Geophys. Res. Lett.* **32**, 1–4 (2005).

12. Barnes, E. A., Polvani, L. M. & Sobel, A. H. Model projections of atmospheric steering of Sandy-like superstorms. *Proc. Natl. Acad. Sci. USA* **110**, 15211–15215 (2013).
13. Bhatia, K. T. et al. Recent increases in tropical cyclone intensification rates. *Nat. Commun.* **10**, 1–9 (2019).
14. Lee, J. et al. Extratropical cyclones over East Asia: Climatology, seasonal cycle, and long-term trend. *Clim. Dyn.* **54**, 1131–1144 (2020).
15. IPCC. Summary for Policymakers in *Climate Change 2021: The Physical Science Basis. Contribution of Working Group I to the Sixth Assessment Report of the Intergovernmental Panel on Climate Change* 1-39 (Cambridge University Press, 2022).
16. Tamarin-Brodsky, T. & Kaspi, Y. Enhanced poleward propagation of storms under climate change. *Nat. Geosci.* **10**, 908–913 (2017).
17. Walker, D. I., Kendrick, G. A. & McComb, A. J. The distribution of seagrass species in Shark Bay, Western Australia, with notes on their ecology. *Aquat. Bot.* **30**, 305–317 (1988).
18. Preen, A. R., Marsh, H., Lawler, I. R., Prince, R. I. T. & Shepherd, R. Distribution and abundance of dugongs, turtles, dolphins and other megafauna in Shark Bay, Ningaloo Reef and Exmouth Gulf, Western Australia. *Wildl. Res.* **24**, 185–208 (1997).
19. Tyne, A. et al. Ecological characteristics contribute to sponge distribution and tool use in bottlenose dolphins Tursiops sp. *Mar. Ecol. Prog. Ser.* **444**, 143–153 (2012).
20. Heron S. F. et al. *Application of the Climate Vulnerability Index for Shark Bay, Western Australia. Western Australian Marine Science Institution, Perth, Western Australia.* https://www.wamsi.org.au/sites/wamsi.org.au/files/HeronEtAl_2020_CVI-SharkBay-report.pdf (2020).
21. Playford, P. E., Cockbain, A. E. Berry, P. F. Haines P. W. & Brooke B. P., *The Geology of Shark Bay* . p. 146(Geological Survey of Western Australia Bulletin, 2013).
22. Kendrick, G. A. et al. Science behind management of Shark Bay and Florida Bay, two P-limited subtropical systems with different climatology and human pressures. *Mar. Freshw. Res.* **63**, 941–951 (2012).
23. Fraser et al. Extreme climate events lower resilience of foundation seagrass at edge of biogeographical range. *J. Ecol.* **102**, 1528–1536 (2014).
24. Arias-Ortiz, A. et al. A marine heatwave drives massive losses from the world's largest seagrass carbon stocks. *Nat. Clim. Change* **8**, 338–344 (2018).
25. Strydom, S. et al. Too hot to handle: unprecedented seagrass death driven by marine heatwave in a World Heritage Area. *Glob. Chang Biol.* **26**, 3525–3538 (2020).
26. Nicholls, N., Landsea, C. & Gill, J. Recent trends in Australian region tropical cyclone activity. *Meteorol* **65**, 197–205 (1998).
27. Bureau of Meteorology. *The Australian Tropical Cyclone Database*. Available at: http://www.bom.gov.au/cyclone/history/index.shtml [accessed 09/09/2020].
28. Bureau of Meteorology. *Report on Cyclone Hazel*. Available at: http://www.bom.gov.au/cyclone/history/hazel.shtml [accessed 09/09/2020]. (2020b).
29. Bureau of Meteorology. *Report on Cyclone Herbie*. Available at: http://www.bom.gov.au/cyclone/history/herbie.shtml [accessed 09/09/2020]. (2020c).
30. Bureau of Meteorology. *Past Tropical Cyclones: Best Track Archive*. Available at: http://www.bom.gov.au/cyclone/tropical-cyclone-knowledge-centre/history/ [accessed 09/09/2020]. (2020d).
31. Shire of Shark Bay. *Local Planning Scheme No 3: District Zoning Scheme*. https://www.sharkbay.wa.gov.au/Profiles/sharkbay/Assets/ClientData/Document-Centre/Public-Documents/Denham-Town-Planning/Town_Planning_Scheme_4_-_2016/Scheme_Review_Explanatory_report.pdf (2012).
32. Foley, G. R. & Hanstrum, B. N. The capture of tropical cyclo.es by cold fronts off the west coast of Australia. *Weather Forecast.* **9**, 577–592 (1994).
33. Courtney, J. B. et al. Revisions to the Australian tropical cyclone best track database. *J. South. Hemisphere Earth Syst. Sci.* **71**, 203–227 (2021).
34. Nott, J. A 6000 year tropical cyclone record from Western Australia. *Q. Sci. Rev.* **30**, 713–722 (2011).
35. Church, J. A., Hunter, J. R., McInnes, K. L. & White, N. J. Sea-level rise around the Australian coastline and the changing frequency of extreme sea-level events. *Aust. Meteorol. Mag.* **55**, 253–260 (2006).
36. Soria, J. L. A. et al. Typhoon Haiyan overwash sediments from Leyte Gulf coastlines show local spatial variations with hybrid storm and tsunami signatures. *Sediment. Geol.* **358**, 121–138 (2017).
37. Haigh, I. D. et al. Estimating present day extreme water level exceedance probabilities around the coastline of Australia: tropical cyclone-induced storm surges. *Clim. Dyn.* **42**, 139–157 (2014).
38. McInnes, K. L., Walsh, K. J. E., Hubbert, G. D. & Beer, T. Impact of sea-level rise and storm surges on a coastal community. *Nat. Hazards* **30**, 187–207 (2003).
39. Lin, N., Emanuel, K. A., Smith, J. A., & Vanmarcke, E. Risk assessment of hurricane storm surge for New York City. *J. Geophys. Res. Atmos.* **115**, 1–18 (2010).
40. Harper, B. A., Stroud, S. A., McCormack, M. & West, S. A review of historical tropical cyclone intensity in northwestern Australia and implications for climate change trend analysis. *Aust. Meteorol. Mag.* **57**, 121–141 (2008).
41. Williamson, F. et al. New directions in hydro-climatic histories: observational data recovery, proxy records and the atmospheric circulation reconstructions over the earth (ACRE) initiative in Southeast Asia. *Geosci. Lett.* **2**, 1–12 (2015).
42. Zhu, Z. et al. Historic storms and the hidden value of coastal wetlands for nature-based flood defence. *Nat. Sustain.* **3**, 1–10 (2020).
43. Torn, R. D. & Snyder, C. Uncertainty of tropical cyclone best-track information. *Weather Forecast.* **27**, 715–729 (2012).
44. Tang, C. K., Chan, J. C. & Yamaguchi, M. Large tropical cyclone track forecast errors of global numerical weather prediction models in western North Pacific basin. *Trop. Cyclone Res. Rev* **10**, 151–169 (2021).
45. Donnelly, J. P. et al. 700 yr sedimentary record of intense hurricane landfalls in southern New England. *Geol. Soc. Am. Bull.* **113**, 714–727 (2001).
46. Wallace, D. J., Woodruff, J. D., Anderson, J. B. & Donnelly, J. P. Palaeohurricane reconstructions from sedimentary archives along the Gulf of Mexico, Caribbean Sea and western North Atlantic Ocean margins. *Geol. Soc. Spec. Publ.* **388**, 481–501 (2014). 2014.
47. Lin, N., Kopp, R. E., Horton, B. P. & Donnelly, J. P. Hurricane Sandy's flood frequency increasing from year 1800 to 2100. *Proc. Natl. Acad. Sci. USA* **113**, 12071–12075 (2016).
48. May, S. M. et al. Traces of historical tropical cyclones and tsunamis in the Ashburton Delta (north-west Australia). *Sedimentology* **62**, 1546–1572 (2015).
49. Bregy, J. C. et al. US Gulf Coast tropical cyclone precipitation influenced by volcanism and the North Atlantic subtropical high. *Commun. Earth Environ.* **3**, 1–11 (2022).
50. Frappier, A. B. et al. Two millennia of tropical cyclone-induced mud layers in a northern Yucatán stalagmite: Multiple overlapping climatic hazards during the Maya Terminal Classic "megadroughts". *Geophys. Res. Lett.* **41**, 5148–5157 (2014).
51. Miller, D. L. et al. Tree-ring isotope records of tropical cyclone activity. *Proc. Natl. Acad. Sci. USA* **103**, 14294–14297 (2006).
52. Collins-Key, S. A. & Altman, J. Detecting tropical cyclones from climate-and oscillation-free tree-ring width chronology of longleaf pine in south-central Georgia. *Glob. Planet. Change* **201**, 103490 (2021).
53. Knapp, P. A., Maxwell, J. T. & Soulé, P. T. Tropical cyclone rainfall variability in coastal North Carolina derived from longleaf pine (Pinus palustris Mill.): AD 1771–2014. *Clim. Change* **135**, 311–323 (2016).
54. Mitchell, T. J., Knapp, P. A. & Ortegren, J. T. Tropical cyclone frequency inferred from intra-annual density fluctuations in longleaf pine in Florida, USA. *Clim. Res.* **78**, 249–259 (2019).
55. Pfister, C. In *The Palgrave Handbook of Climate History* (pp. 37-47) (Palgrave Macmillan, 2018).
56. Herrera, R. G. et al. The use of Spanish and British documentary sources in the investigation of Atlantic hurricane incidence. *Hurricanes and Typhoons: Past, Present, and Future*. pp149 (Columbia University Press, 2004).
57. Terry, J. P., Winspear, N. & Cuong, T. Q. The 'terrific Tongking typhoon' of October 1881–implications for the Red River Delta (northern Vietnam) in modern times. *Weather* **67**, 72–75 (2012).
58. Chan, J. C., Liu, K. S., Xu, M. & Yang, Q. Variations of frequency of landfalling typhoons in East China, 1450-1949. *Int. J. Climatol.* **32**, 1946–1950 (2012).
59. Soria, J. L. A. et al. Repeat storm surge disasters of Typhoon Haiyan and its 1897 predecessor in the Philippines. *Bull. Am. Meteorol. Soc* **97**, 31–48 (2016).
60. Hunt, H. A. *Results of Rainfall Observations Made In Western Australia Including All Available Annual Rainfall Totals From 1374 Stations For All Years Of Record Up To 1927, With Maps And Diagrams* (Bureau of Meteorology, 1929).
61. Christensen, J. Willy-willies of the Old Northwest. *J. R. Soc. West. Aust.* **103**, 113–128 (2019).
62. Daily News Perth, 26 February p5. https://trove.nla.gov.au/newspaper/page/7977214 (1921).
63. Zerger, A., Smith, D. I., Hunter, G. J. & Jones, S. D. Riding the storm: a comparison of uncertainty modelling techniques for storm surge risk management. *Appl. Geogr.* **22**, 307–330 (2002).
64. Zhong, L., Li, M. & Zhang, D. L. How do uncertainties in hurricane model forecasts affect storm surge predictions in a semi-enclosed bay? *Estuar. Coast. Shelf Sci.* **90**, 61–72 (2010).
65. Lin, N. & Chavas, D. On hurricane parametric wind and applications in storm surge modeling. *J. Geophys. Res. Atmos.* **117**, D09120 (2012).
66. Garzon, J. L. & Ferreira, C. M. Storm surge modeling in large estuaries: sensitivity analyses to parameters and physical processes in the Chesapeake Bay. *J. Mar. Sci. Eng.* **4**, 45 (2016).
67. Faivre, G., Burston, J. M., Ware, D. & Tomlinson, R. Queensland storm surge forecasting model design using sensitivity analysis. *21st International Congress on Modelling and Simulation, Gold Coast, Australia,* (Modelling & Simulation Society of Australia & New Zealand, 2015).

68. Holland, G. J., Belanger, J. I. & Fritz, A. A revised model for radial profiles of hurricane winds. *Mon. Weather Rev.* **138**, 4393–4401 (2010).
69. Burston, J. M., Taylor, D. R. & Churchill, J. W. Stochastic tropical cyclone modelling in the Australian region: An updated track model. *Proceedings of the Australasian Coasts and Ports Conference, September 2015, Auckland, New Zealand.* Engineers Australia (2015).
70. Burston, J. M., Taylor, D. R., Dent, J. M. & Churchill, J. W. Australia-wide tropical cyclone multi-hazard risk assessment. *Proceedings of the Australasian Coasts and Ports Conference*, Engineers Australia (2017).
71. Deltares. Delft3D-Flow, Simulation of multi-dimensional hydrodynamic flows and transport phenomena, including sediments, *User Manual*, Version 3.15.34158, Deltares, May 2014, p. 684 (2014).
72. Deltares. Delft3D Flexible Mesh Suite, *D-Flow FM in Delta Shell, User Manual*, Version 1.1.148, Deltares, November 2015, p. 376 (2015).
73. Churchill, J. W., Taylor, D. R., Burston, J. M. & Dent, J. M. *Assessing Storm Tide Hazard for the North-West Coast of Australia using an Integrated High-Resolution Model System. 1st International Workshop on Waves, Storm Surges and Coastal Hazards – Liverpool, UK,* National Oceanography Centre *10-15 September 2017* (2017).
74. Treloar, P., Taylor, D. & Prenzler, P. *Investigation Of Wave Induced Storm Surge Within a Large Coastal Embayment - Moreton Bay (Australia). Coast. Eng. Proc*., Coastal Engineering Research Council *1*, currents. 22. (2011).
75. Smith, M., Couper, Z., Teakle, I. & Metters D., Storm Tide in a Data Rich Coastal Embayment, Finding the Missing Storm Surge. *Proceedings of 37th International Conference on Coastal Engineering*. Sydney, Australia, Coasts, Oceans, Ports, and Rivers Institute (COPRI) Dec 2022 (2022).
76. Bureau of Meteorology: Severe tropical cyclone Vance, http://www.bom.gov.au/cyclone/history/vance.shtml (last access: 20 June 2020), (2011).
77. Nott, J. & Hubbert, G. Comparisons between topographically surveyed debris lines and modelled inundation levels from severe tropical cyclones Vance and Chris, and their geomorphic impact on the sand coast. *Aust. Meteorol. Mag.* **54**, 187e196 (2005).
78. Queensland Government. Tropical Cyclone Yasi - 2011 *Post Cyclone Coastal Field Investigation. Queensland Department of Science, Information Technology, Innovation and the Arts, Brisbane, Australia*. Available online at www.longpaddock.qld.gov.au/about/publications/index.html (2012).
79. Ginger, J., Henderson, D., Edwards, M. & Holmes, J. Housing damage in windstorms and mitigation for Australia. In *Proceedings of the APEC-WW & IG-WRDRR Joint Workshop on Wind-Related Disaster Risk Reduction (WRDRR)*, (International Association for Wind Engineering, 2010).
80. Shire of Shark Bay. *Denham Inundation Levels Storm Surge Modelling Report*. Denham: M.P. Rogers and Associates on behalf of: Shire of Shark Bay. R558 Rev0 (2014).
81. Christensen, J. & Jones, R. World Heritage and local change: conflict, transformation and scale at Shark Bay, Western Australia. *J. Rural Stud.* **74**, 235–243 (2020).
82. Christensen, J. *Pearls, People and Power: Pearling and the Indian Ocean Worlds* (eds. P. Machado, S. Mullins and J. Christensen) (University Press, 2020).
83. McKenzie, L. J., Collier, C. J. & Waycott, M., 2012. *In: Reef Rescue Marine Monitoring Program: Nearshore Seagrass, Annual Report for the sampling period 1st July 2010–31st May 2011*. p. 177 (Fisheries Queensland, 2012).
84. Beeden, R. et al. Impacts and recovery from severe tropical Cyclone Yasi on the Great Barrier Reef. *PLoS ONE* **10**, e0121272 (2015).
85. Rasheed, M. A., McKenna, S. A., Carter, A. B. & Coles, R. G. Contrasting recovery of shallow and deep water seagrass communities following climate associated losses in tropical north Queensland, Australia. *Mar. Poll. Bull.* **83**, 491–499 (2014).
86. Kilminster, K. et al. Unravelling complexity in seagrass systems for management: Australia as a microcosm. *Sci. Total Environ.* **534**, 97–109 (2015).
87. Sobtzick, S., Aerial survey of the urban coast of Queensland to evaluate the response of the dugong population to the widespread effects of the extreme weather events of the summer of 2010-11. *Reef and Rainforest Research Centre Limited*. p63 (2012).
88. Nowicki, R. et al. Indirect legacy effects of an extreme climatic event on a marine megafaunal community. *Ecol. Monogr.* **89**, e01365 (2019).
89. NESP Earth Systems and Climate Change Hub. Climate change and the Shark Bay World Heritage Area: foundations for a climate change adaptation strategy and action plan, *Earth Systems and Climate Change Hub Report No. 7*, NESP Earth Systems and Climate Change Hub, Australia. (2018).
90. Kossin, J. P., Emanuel, K. & Vecchi, G. A. The poleward migration of the location of tropical cyclone maximum lifetime intensity. *Nature* **509**, 349–352 (2014).
91. Lavender, S. L. & Walsh, K. J. E. Dynamically downscaled simulations of Australian region tropical cyclones in current and future climates. *Geophys. Res. Lett.* **38**, L10705 (2011).
92. Brázdil, R., Kiss, A., Luterbacher, J., Nash, D. J. & Řezníčková, L. Documentary data and the study of past droughts: a global state of the art. *Clim. Past* **14**, 1915–1960 (2018).
93. Nott, J., Green, C., Townsend, I. & Callaghan, J. The world record storm surge and the most intense southern hemisphere tropical cyclone: new evidence and modeling. *Bull. Am. Meteorol. Soc.* **95**, 757–765 (2014).
94. Kelso, C. & Vogel, C. The climate of Namaqualand in the nineteenth century. *Clim. Change* **83**, 357–380 (2007).
95. Nash, D. J. et al. Climate indices in historical climate reconstructions: a global state of the art. *Clim. Past* **17**, 1273–1314 (2021).
96. Navy, R. A. *Hydrographic Service.* (Royal Australian Navy, 2020).
97. Stammer, D. et al. Accuracy assessment of global barotropic ocean tide models. *Rev. Geophys.* **52**, 243–282 (2014).
98. Shea, D. J. & Gray, W. M. The hurricane's inner core region. I. Symmetric and asymmetric structure. *J. Atmos. Sci. 30* **8**, 1544–1564 (1973).
99. Sobey, R. J., Harper, B. A. & Stark, K. P. *Numerical Simulation of Tropical Cyclone Storm Surge*. Department of Civil and Systems Engineering, Research Bulletin No. CS14, May, p. 300 (James Cook University, 1977).
100. Lowe, R. J., Cuttler, M. V. W. & Hansen, J. E. Climatic drivers of extreme sea level events along the coastline of Western Australia. *Earth's Future* **9**, e2020EF001620 (2021).
101. Vijayan, L. et al. Evaluation of parametric wind models for more accurate modeling of storm surge: a case study of Hurricane Michael. *Nat. Hazards* **106**, 2003–2024 (2021).
102. Knapp, K. R., Kruk, M. C., Levinson, D. H., Diamond, H. J. & Neumann, C. J. The international best track archive for climate stewardship (IBTrACS) unifying tropical cyclone data. *Bull. Am. Met. Soc.* **91**, 363–376 (2010).

Acknowledgements

The authors acknowledge the Malgana Peoples as the traditional custodians of Gath-aagudu, and pay respects to their Elders past, present and emerging. A.D.S. and J.C. (at Murdoch University) were assisted by Australian Research Council LP150100649 and J.C. by the Social Sciences and Humanities Research Council of Canada. A.D.S. was supported by the Singapore Ministry of Education Academic Research Fund MOE2019-T3-1-004 and Earth Observatory of Singapore (grant no. 003113-00001) via its funding from the National Research Foundation Singapore and the Singapore Ministry of Education under the Research Centres of Excellence initiative. The authors acknowledge HOLSEA and PALSEA, working groups of the International Union for Quaternary Sciences (INQUA) and Past Global Changes (PAGES), which in turn received support from the Swiss Academy of Sciences and the Chinese Academy of Sciences. MWF was supported by the Robson and Robertson Research Fellowship awarded by UWA, and the Integrated Coastal Analyses and Sensor Technology (ICoAST) project with funding from the Indian Ocean Marine Research Centre, a joint partnership between UWA, AIMS, CSIRO and DPIRD WA. This article is a contribution to International Geoscience Program (IGCP) Project 725, "Forecasting Coastal Change: From Cores to Code." This work comprises EOS contribution number 524. The authors thank Constance Chua for comments on an earlier draft, Fiona Williamson for comments on the QHDF and Emma Hill for comments on Inverse modelling.

Author contributions

A.D.S. led the conceptualisation, methodology, formal analysis, writing of original draft, reviewing and editing; J.C. led the development of the QHDF and the data sourcing and compilation of historical datasets along with the writing, reviewing and editing. J.A. and D.T. led the modelling component of the program with contributions to the model from Jim Churchill and Holly Watson. M.W.F. and J.S. led the work on ecosystem impacts, provided local context and contributed to the writing of original draft.

Competing interests

A.D.S. is an Editorial Board Member for Communications Earth & Environment, but was not involved in the editorial review of, nor the decision to publish this article. All other authors have no competing interests.

Additional information

Supplementary information The online version contains supplementary material available at https://doi.org/10.1038/s43247-023-00844-z.

Correspondence and requests for materials should be addressed to Adam D. Switzer.

Peer review information *Communications Earth & Environment* thanks Ning Lin and the other, anonymous, reviewer(s) for their contribution to the peer review of this work. Primary Handling Editor: Joe Aslin. A peer review file is available